IEEE Access
Multidisciplinary | Rapid Review | Open Access Journal

Received February 3, 2021, accepted February 10, 2021, date of publication February 16, 2021, date of current version March 8, 2021.

Digital Object Identifier 10.1109/ACCESS.2021.3059665

Solving of Optimal Power Flow Problem Including Renewable Energy Resources Using HEAP Optimization Algorithm

MOHAMED A. M. SHAHEEN[1], HANY M. HASANIEN[2], (Senior Member, IEEE), AND AHMED AL-DURRA[3], (Senior Member, IEEE)

[1]Electrical Engineering Department, Faculty of Engineering and Technology, Future University in Egypt, Cairo 11835, Egypt
[2]Electrical Power and Machines Department, Faculty of Engineering, Ain Shams University, Cairo 11517, Egypt
[3]Advanced Power and Energy Center, Department of Electrical Engineering and Computer Science, Khalifa University, Abu Dhabi 127788, United Arab Emirates

Corresponding author: Ahmed Al-Durra (ahmed.aldurra@ku.ac.ae)

This work was supported by the Advanced Power and Energy Centre (APEC) at Khalifa University of Science and Technology, Abu Dhabi, UAE, under Grant APEC-06-2018.

ABSTRACT This paper presents a novel endeavor to use the Heap optimization algorithm (HOA) to solve the problem of optimal power flow (OPF) in the electricity networks. The key objective is to optimize the cost of fuel of the conventional generators under the system limitations. Various scenarios are studied in a later stage considering the addition of the PV panel and/or wind farm with changing load curves during a typical day. The active output power of the generators is selected to be the OPF problem search space. The HOA is employed to get the best solution of the fitness function and provides the corresponding best solutions. The modeling of the heap-based optimizer (HBO) depends on three levels: the relation between the subordinates and the boss, the relation between the same level employees, and the contribution of the employee oneself. The validity of the proposed algorithm is tested for a variety of electric grids, the IEEE 30-bus, IEEE 57-bus and 118 bus networks. These networks are simulated under various scenarios. Real load curves, in this study, are considered to achieve a practical outcome. The simulation outcomes are evaluated and tested. The results indicate that the implemented HOA-based OPF methodology is flexible and applicable compared with that achieved by using the genetic algorithm.

INDEX TERMS Optimal power flow, optimization, power systems, renewable energy.

I. INTRODUCTION

A. MOTIVATION AND INCITEMENT

Power systems are known as dynamic systems with a high degree of complexity. They consist of generation stations, transmission networks, and distribution networks that are owned and managed by companies or countries. The electric power transmission grids have some limitations while operation. These limitations emerge from issues about temperature, voltage and stability [1]. The OPF problem is a well-known nonlinear optimization problem. The main objective of the OPF optimization problem is to choose the optimal solution for the network or grid design variables that meet the minimum value of the objective function taking into account the constraints of the electric power system. The active generator power, generator voltage, transformer taps settings or VAR compensators can be described as a design variable by the researchers. Generally, the OPF objective functions are categorized according to a single objective function or multi-objective functions. In the single objective function optimization problems, only one objective is targeted meanwhile in the multi-objective ones, many objectives are accomplished simultaneously. These targets can include the generators' fuel costs, the generators' emission rates, electricity loss in an electricity grid and the voltage security index.

B. LITERATURE REVIEW

The OPF problem was dedicated by more than one traditional method in the literature survey like the Newton–Raphson [2], and the interior point method [3]. Orthodox

The associate editor coordinating the review of this manuscript and approving it for publication was S. Ali Arefifar.

This work is licensed under a Creative Commons Attribution 4.0 License. For more information, see https://creativecommons.org/licenses/by/4.0/

approaches typically suffer from several demerits. The initial problem guess that depends on the differential equation solver which is heavily impacted on them. Furthermore, because the OPF optimization problem is nonlinear, the traditional methods can be kept in the local minimum point instead of the global minimum. Furthermore, the problems must be simplified by specifying mathematical assumptions. Therefore, to overcome such drawbacks and obstacles, it is necessary to find competent methods of optimization.

Different innovative metaheuristic methods are recently used to handle the OPF. These methods were successful in removing barriers of conventional mathematical methods. Particle swarm optimization (PSO) [4], grey wolf optimization and differential evolution [5], [6], tree-seed algorithm [7], sine-Cosine algorithm [8], sun-flower optimization (SFO) [9], [10], coyote optimization algorithm [11], harris-hawks optimization (HHO) [12], [13], cuttlefish algorithm [14], cuckoo search algorithm [15], whale-optimization algorithm (WOA) [16], gravitational-search [17], marine predators [18], and salp swarm algorithm [19]–[22] are naturally inspired and divided fundamentally in techniques based on swarms and population. They have both their own benefits and inconvenience individually [23]. These metaheuristic-based methods initiate hazardous candidates and achieve the best solution based on their operation.

A community of individuals who work for a shared purpose will not do so until they organize themselves into a hierarchy known as a Corporate Rank hierarchy (CRH). This is the idea of proposing a new optimization algorithm, which arranges the fitness of search agents in a hierarchy. As the heap data structure is used to map a CRH definition, the algorithm proposed is called a heap optimization algorithm (HOA). This algorithm was first introduced by Qamar Askari, Mehreen Saeed, and Irfan Younas in 2020 [24]. Regarding the modeling of the HOA mathematically, it consists of three pillars: the combination of subordinates with the direct supervisor, the relationship amongst peers and the employee's own participation. The results are either higher or similar to the other algorithms used in literature. The novel meta-heuristic algorithm is motivated by such social behaviors, since the extraordinary outcomes of human behavioral optimization methods have pushed the domain of evolutionary-based and swarm-based intelligence up to a higher level. The proposed algorithm smartly models three forms of worker behavior: for example, subordinates' interaction with their immediate head, colleague-to-work interaction and employee self-contribution. The proposed optimization method may be updated to handle number of problems with smart systems related to engineering, industry, research and business optimization. The HOA allows many real-life resource planning, manufacturing planification, automobile steering, network optimization, robotics track preparation, packaging issues, and intelligent systems architecture challenge to be solved. Furthermore, The HOA is simple in design and implementation [24].

C. CONTRIBUTION AND PAPER ORGANIZATION

The OPF remains active and continues with the use of these approaches as novel metaheuristic strategy development. It has multiple goals. It can be solved simultaneously and/or in sequence. The most common aim is to minimize the fuel cost of the generators. The HOA is used to deal with the OPF in this article. The proposed method is designed to minimize a single target within the network constraints. The research has in fact provided: (1) measurement of the proficiency and success of the HOA when handling the OPF in power systems compared with obtained using the genetic algorithm (GA), (2) optimum photovoltaic (PV) [25] and wind farm positioning [26] using the sunflower optimization (SFO) and the Harris Hawks Optimization (HHO) algorithm, and (3) impact of adding PV and/or wind turbines [27] on the cost of fuel in the OPF using the proposed HOA compared with the GA [28]. The goal is to minimize fuel prices. The algorithm adopted is used for evaluating the best values for the variables of the architecture regulation. The real output power of the generators is the OPF search space. The HOA is chosen for the OPF in the electric grids, the standard IEEE 30-, 57- and 118-bus systems considering many scenarios. Real load curves are considered in this analysis to achieve a practical outcome. The results of optimization are provided by MATLAB software, and the results obtained illustrate the HOA's competition to reach the OPF optimization problem solution with GA. The major contributions of this paper are: 1) Evaluation of the newly proposed HOA when applied to the OPF problem in its classical base case, 2) Investigating the effect of inserting renewable energy sources and load variation through a typical day of the objective function to be minimized.

The remaining sections of the paper are organized as follows: Section 2 presents the problem formulation. Section 3 presents the proposed algorithm employed for solving the OPF problem with different scenarios. Section 4 presents a discussion on the simulation results. Finally, the conclusion is presented in Section 5.

II. FORMULATION OF THE OPF

Firstly, the goal is to make an assessment to the newly developed HOA with the help of the MATPOWER to run the OPF in the base case, without adding renewable energy sources and with fixed load, comparing the results with GA. Secondly, the optimum location where PV-panels are to be installed is decided by the SFO and HHO algorithms [9], [13]. The wind farm is positioned at an optimal bus. Thirdly, the OPF problem can be solved after only PV panels are inserted, only then a wind farm. Then, the OPF is tested concurrently with the addition of PV panels and wind farm. The networks that are used for this analysis, the standard IEEE 30-, 57-, and 118- bus systems.

A. OPF WITH BASE CASE

The problem is an OPF single objective optimization problem. The following subsection clarifies it.

1) THE SINGLE OBJECTIVE

The prices charged by the energy services are the running costs of generators, which often cost of fuel during the operation. The cost function is defined in equations (1) and (2) as a quadratic function for the output active power [9].

$$Minimize\ \ J = \sum_{h=1}^{24}\sum_{i=1}^{NG} C_{i,h}\left(P_{Gi,h}\right) \tag{1}$$

$$C_{i,h}\left(P_{Gi,h}\right) = a_i * P_{Gi,h}^2 + b_i * P_{Gi,h} + c_i \tag{2}$$

where $\boldsymbol{J}$ stands for the cost charged by the service provider, $\boldsymbol{NG}$ represents the number of generators, and $\boldsymbol{P_{Gi,h}}$ represents the real power at bus $\boldsymbol{i}$ and moment $\boldsymbol{h}$.

2) OPF PROBLEM CONSTRAINTS

The limitations of the OPF are expressed as shown in the following equations [9]:

$$P_{injk,h} - \sum_{l=1}^{N} V_{k,h} * V_{l,h} * \left[G_{kl} * \cos\left(\delta_{l,h} - \delta_{k,h}\right) + B_{kl} * \sin\left(\delta_{l,h} - \delta_{k,h}\right)\right] = 0 \tag{3}$$

$$Q_{injk,h} - \sum_{l=1}^{N} V_{k,h} * V_{l,h} * \left[G_{kl} * \sin\left(\delta_{l,h} - \delta_{k,h}\right) + B_{kl} * \cos\left(\delta_{l,h} - \delta_{k,h}\right)\right] = 0 \tag{4}$$

where: $P_{injk,h}$, $Q_{injk,h}$ represent the real and reactive power injected at bus k at moment h respectively, $V_{k,h}$ and $V_{l,h}$ represent the voltages of buses k and l at moment h. G_{kl} and B_{kl} represent the conductance and susceptance of Y_{kl}. $\delta_{l,h}$ and $\delta_{k,h}$ represent the voltage angles at buses k and l at hour h respectively.

$$P_{Gmin} \leq P_{Gi,h} \leq P_{Gmax},\ i = 1, 2, \ldots, NG\ and\ h = 1, 2, \ldots, 24 \tag{5}$$

$$Q_{Gmin} \leq Q_{Gi,h} \leq Q_{Gmax}, i = 1, 2, \ldots, NG\ and\ h = 1, 2, \ldots, 24 \tag{6}$$

$$V_{imin} \leq V_{i,h} \leq V_{imax},\ i = 1, 2, \ldots, NG\ and\ h = 1, 2, \ldots, 24 \tag{7}$$

$$\left|V_{k,h} * V_{l,h} * \left[G_{kl} * \cos\left(\delta_{l,h} - \delta_{k,h}\right) + B_{kl} * \sin\left(\delta_{l,h} - \delta_{k,h}\right)\right]\right| \leq P_{limkl}, k,\ l = 1, 2, \ldots, N \tag{8}$$

where P_{limkl} represents the maximum power flow of a branch between nodes k and l.

B. TARGETING THE OPTIMAL BUSES OF THE RENEWABLE ENERGY SOURCES

The OPF is performed to add the PV panels starting trials at bus 2 until the end of the whole buses of each system, one at a time [9]. The bus that results in a lower cost for 24 hours is the best-chosen bus to add PV panels. The OPF is also run to optimize the wind farm location following the same strategy of the PV panel optimal siting, providing that the PV panel is mounted on the earlier chosen buses. In this study, the PV panel is selected to be of 15 MW capacity and the wind farm is 30 MW when studying the 30-bus system. For the 57-bus system, the added PV panel is selected to be of 90 MW capacity and the wind farm capacity is selected to be 175 MW. Finally, the PV added to the 118-bus system has a capacity of 300 MW while the added wind farm is a 575 MW one. These capacities are chosen to be comparable with the maximum demands of the test systems. In general, The PV panel and the wind farm produce a time varying electric power through the day [29], [30], [31]. The hourly power generated by the PV panel and the wind farm in a typical day in winter is shown in Fig. 1 [9].

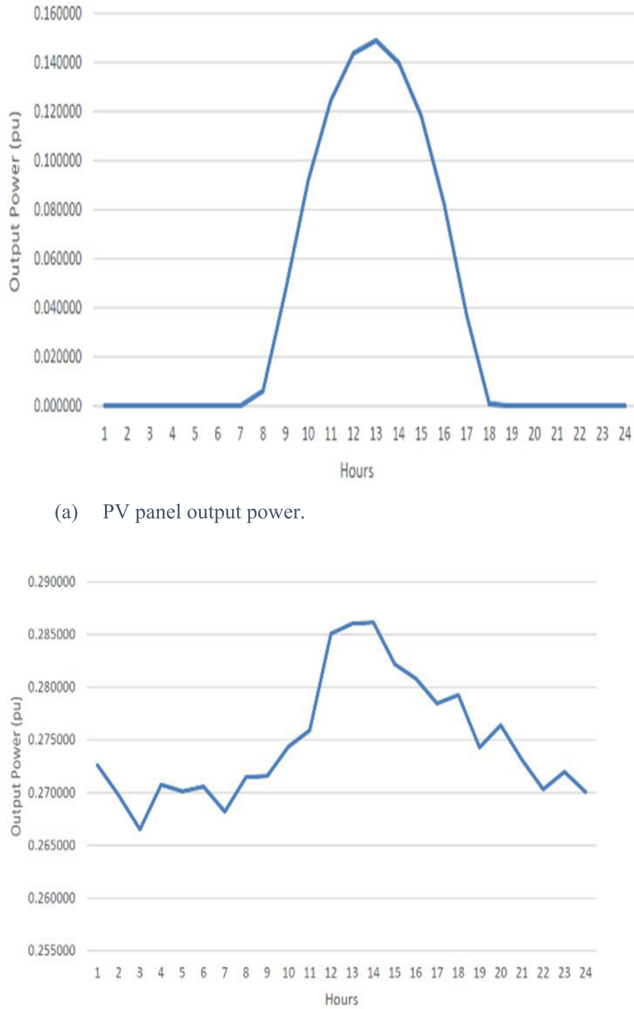

(a) PV panel output power.

(b) Wind farm output power.

FIGURE 1. Hourly power provided by (a) PV panel, (b) Wind farm.

C. OPF INCLUDING VARIABLE LOADING CONDITIONS AND RENEWABLE ENERGY SOURCES

Following allocation of PV panels and wind turbines, the effects of incorporating these green energy sources on the overall cost of the OPF are evaluated in various scenarios. First of all, the only solar energy supplier is added to the OPF and then the only wind farm is added. The OPF is then performed corresponding to PV and wind power sources addition and saves the right solution in each situation. The independent control parameter is the active power taken from the generator and the HOA as represented in Eq. (5) holds it within its borders. The limits of the equalities represented in Eq. (3), (4), and (6) are fulfilled with the use of MATPOWER toolbox [32] and the MATLAB environment with the Newton-Raphson power flow. The inclusion of penalty factors is to satisfy the objective without constraint violations, limits the other dependent variables. These penalties are represented mathematically in Eq. (9) [9].

$$\begin{aligned} Penalties = K_v \sum\nolimits_{i=1}^{N} \Big[\max\left(0, V_i - V_i^{max}\right) \\ + \max\left(0, V_i^{min} - V_i\right)\Big] \\ + K_l \sum\nolimits_{j=1}^{nbr} \Big[\max\left(0, S_j - S_j^{rated}\right) \end{aligned} \tag{9}$$

where K_v and K_l are great positive numbers.

III. THE HOA

In organizations, the employees are grouped under a hierarchy that can be named CRH, a form of social contact among people can be seen. This rises the administrative structures such that people can accomplish the corporate objectives effectively. A treelike arrangement is the hierarchy of businesses. The supervisor is assigned to the highest level and the workers are assigned to the parent-child nodes. Subordinates are responsible for communicating their immediate supervisor. People on the same stage are the colleagues.

A. INSPIRATION

The framework of the organization is a collection of strategies that organize the task. This system has aimed at arranging the tasks and meeting the final aims in an optimum way.

The definition is divided into four steps:

- CRH modeling,
- Modeling the relationship between assistants and the head,
- Modeling the relationship between the colleagues,
- Modeling an employee self-contribute to a job.

B. MODELING THE CRH

Given the existence of CRH, the Heap Data Structure is used as a basis for CRH. The entire CRH is the population. A search agent is the heap node during the deployment process. The key to the node in this heap is the fitness of the population and the search agent index in the population is known to be the heap node. A heap data structure of the method of CRH modelling is more illustrated in Fig. 2 [24].

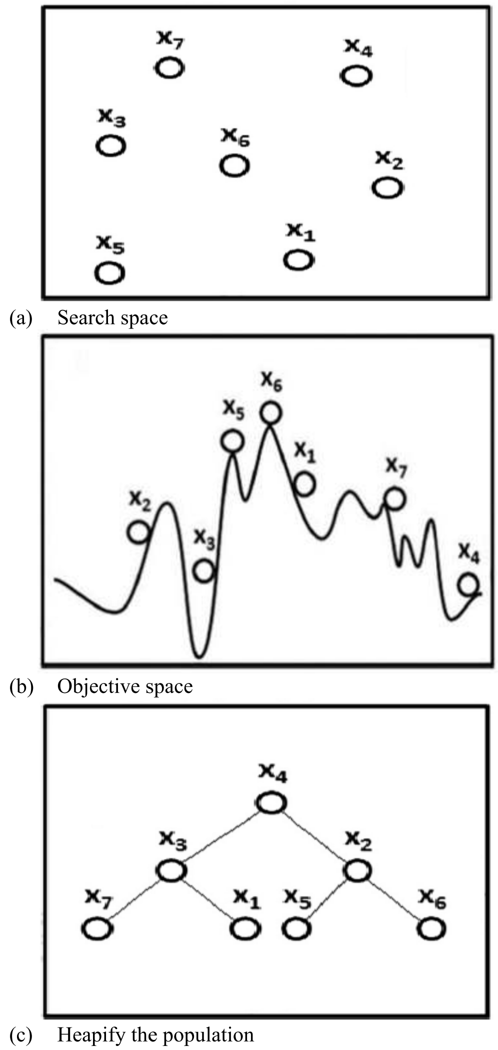

FIGURE 2. Modeling of the CRH with min-heap, (a) Search space, (b) Objective space, (c) Heapify the population.

C. MODELING OF THE COLLABORATION WITH THE BOSS

Regulations are implemented in a structured hierarchical system of the highest ranks and subordinates obey their supervisor. This action is modeled, by modifying the location of the candidate $\vec{x}_i$ with regard to the parent node B, by eq. (10). Each parent node is a supervisor for its children [24]:

$$x^i(t+1) = B^k + \gamma \lambda^k |B^k - x_i(t)| \tag{10}$$

where t is the ongoing iteration, $k$is the kth component of a vector. λ^k represents the kth component of vector $\vec{\lambda}$. It's calculated as in eq. (11) [24]:

$$\lambda^k = 2r - 1 \tag{11}$$

where r is random number between [0], [1].λ is calculated as in eq. (12) [24]:

$$\gamma = \left| 2 - \frac{\left(t \bmod \frac{T}{C}\right)}{\frac{T}{4C}} \right| \tag{12}$$

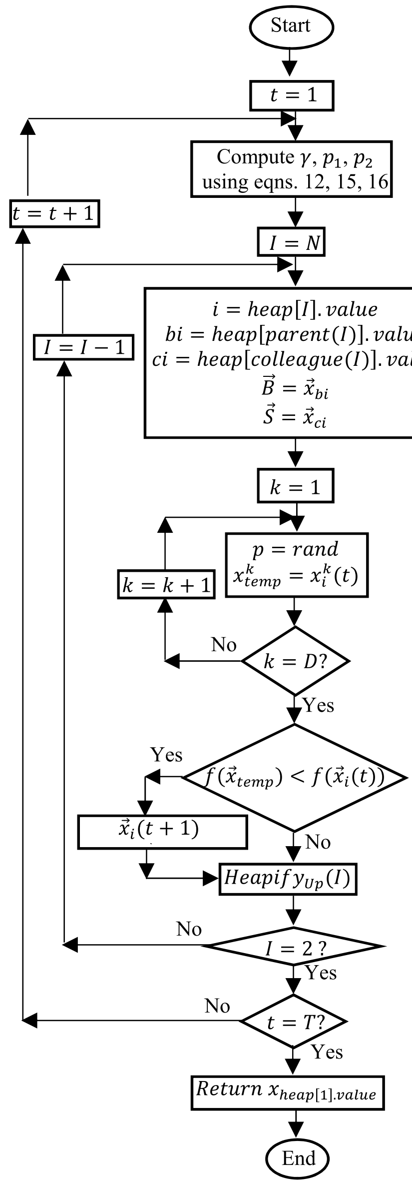

FIGURE 3. Flow chart of the HOA algorithm.

where T is the maximum iterations. C is a parameter that determines the number of cycles γ in T iterations. Through the iterations, γ decreases linearly from 2 to 0. After it equals 0, it increases again to 2.

D. MODELING OF THE COLLABORATION BETWEEN COLLEAGUES

The colleagues collaborate and execute the official duties. In a heap, the same level nodes are colleagues. Accordingly, a population $\vec{x}_i$ modifies its position with respect to a colleague $\vec{S}_r$. This is represented in eq. (13) [24]:

$$x_i^k(t+1) = \begin{cases} S_r^k + \gamma\lambda^k \left|S_r^k - x_i^k(t)\right|, & f\left(\vec{S}_r\right) < f(\vec{x}_i(t)) \\ x_i^k + \gamma\lambda^k \left|S_r^k - x_i^k(t)\right|, & f(\vec{S}_r) \geq f(\vec{x}_i(t)) \end{cases} \tag{13}$$

where f is the fitness function. The randomness in colleagues' selection integrates the search around fit candidates, which enhances the exploitation process.

E. MODELING OF AN EMPLOYEE SELF-CONTRIBUTION

This process simulates an employee self-impact. It is charted simply with some variants suggestions. It is modelled by maintaining the employee's former position into the upcoming iteration, as expressed in eq. (14) [24]:

$$x_i^k(t+1) = x_i^k(t) \tag{14}$$

The population $\vec{x}_i$ keeps its position for the kth control variable for the upcoming iteration.

F. PUTTING ALL TOGETHER

The challenge is to determine the selection probabilities for the three equations to balance exploration and exploitation processes. A roulette wheel is intended to balance the probabilities. It is divided into three parts p_1, p_2, and p_3. The selection of p_1 makes a population to modify the position. The p_1 is limited by eq. (15) [24]:

$$p_1 = 1 - \frac{t}{T} \tag{15}$$

The p_2 is limited by eq. (16):

$$p_2 = p_1 + \frac{1 - p_1}{2} \tag{16}$$

Finally, p_3 is computed as in eq. (17):

$$p_3 = p_2 + \frac{1 - p_1}{2} = 1 \tag{17}$$

The updating mechanism of the HOA is expressed in eq. (18) [24]:

$$x_i^k(t+1) = \begin{cases} x_i^k(t), p \leq p_1 \\ B^k + \gamma\lambda^k \left|B^k - x_i^k(t)\right|, \\ \quad p > p_1 \text{ and } p \leq p_2 \\ S_r^k + \gamma\lambda^k \left|S_r^k - x_i^k(t)\right|, \\ \quad p > p_2 \text{ and } p \leq p_3 \text{ and } f\left(\vec{S}_r\right) < f(\vec{x}_i(t)) \\ x_i^k + \gamma\lambda^k \left|S_r^k - x_i^k(t)\right|, \\ \quad p > p_2 \text{ and } p \leq p_3 \text{ and } f(\vec{S}_r) \geq f(\vec{x}_i(t)) \end{cases} \tag{18}$$

where p is a number between [0], [1].

G. IMPLEMENTATION OF THE HOA

The time and complexity of the introduced method are not influenced by using the heap into the implementation of HOA. The flow chart of the proposed HOA optimization method is shown in Fig. 3.
where i is the index the population P of the I^{th} node. bi and ci are the parent and colleague indices, respectively. $\vec{B}$ and $\vec{S}$ are the parent and colleague position vectors, respectively.

TABLE 1. Key features of the three studied systems.

Number of	IEEE 30	IEEE 57	IEEE 118
buses	30	57	118
generators	6	7	54
branches	41	80	186
transformers	4	17	9
loads	21	42	99
connected loads (MVA)	283.4+j126.2	1250+j336.4	4242+j1438
Load losses (MVA)	5.28+j23.14	16+j72.97	132.86+j783.79

TABLE 2. Simulation parameters of HOA and GA.

		IEEE test system		
		30-bus	57-bus	118-bus
Simulation Time (s)	HOA	348.3	381.5	1880.4
	GA	528.6	11002	4006.3
	PSO	332.3	125.93	-
	MPA	299.1043	763.11663	-
	HHO	-	2095.25	14717.87

TABLE 3. Optimal fitness and population values for the base case OPF for system 1.

Generator power (MW) at bus	HOA	GA	PSO [9]	MPA
1	227.5524643	205.8909	197.89	197.253246
2	20	27.36848	49.98	44.8174083
13	16.65898938	18.92830	15	20.3995709
22	10	14.46586	10	10.0155727
23	10	12.85073	10.015	10
27	12	15.04132	12	12
Min cost($/hr)	906.38723695	914.0514	917.93	915.78184

1) STEPS OF THE PROPOSED HOA

1) Parameters Definition.
2) Population Initialization.
3) Heap building (parent, child, depth, colleague, and Heapify_Up).
4) The heap key and value save the fitness and the population that corresponds the fitness, respectively.

Populations modify the locations to converge on the best solution.

IV. DISCUSSION ON THE SIMULATION RESULTS

This paper introduces the OPF solved using the proposed HOA. To analyse the validity of the proposed HOA-based OPF, the standard IEEE 30-, 57- and 118- bus networks are used. Table 1 presents the key characteristics of the three systems under study. Systems 1, 2, and 3 stands for the IEEE 30-, 57- and 118-bus test systems, respectively.

TABLE 4. Optimal fitness and population values for the base case OPF for system 2.

Generator power (MW) at bus	HOA	GA	PSO [9]	HHO [13]	MPA
1	144.85604 92	151.439 44	153.41	144.89	144.856
2	93.037837 6	85.6551 55	0	94.85	93.0378
3	45.209045 3	47.3166 27	47.07	45.08	45.209
6	68.262358 65	63.8144 1	61.09	65.9	68.2623 5
8	457.02678 2	471.129 09	550	457.17	457.026 7
9	95.856525 1	75.2683 25	89.58	96.009	95.8565
12	365.95697 2	375.581 31	374.31	366.24	365.956 97
Min cost($/hr)	41872.903 23	41891.3 742	42262. 61	41873.0 6	41872.9 03

The design variables of the OPF are the active output power from the generators. The objective is targeted sequentially as explained in the upcoming sections:

A. OPF (THE BASE CASE)

The meant by the base case is the case without insertion of any green energy sources, the OPF is performed on the standard IEEE 30-, 57-, 118- bus test networks. The maximum and minimum boundaries of the control variables of the three systems under study are found in [32]. The number of iterations is chosen to be the stopping criteria of the simulation and the point of the comparison between the HOA and GA. In the IEEE 30-, 57-, 118-bus systems, the maximum numbers of iterations are 600, 5000, 20000, respectively. The objective is the fuel cost minimization. For the three systems studied and all scenarios, the values of the bus voltage and the line flow penalty factors are 9×10^{15} and 9×10^{13}, respectively. A relation between the proposed HOA and GA with respect to the simulation time is seen in Table 2. It can be noted that the HOA needs much lower time than the GA to finish the simulation process. Further data of the dependent variables (Transmission Line apparent power and the Generator reactive power) is attached at the end of this paper after the conclusion section.

For more detailed results, Tables 3-5 are presented to obtain the control variables that correspond the optimal values of the fitness function for the three standard test systems, the IEEE 30-, 57-, and 11-bus test systems, respectively. The figures of the convergence curves of the fitness function are provided with the three test systems. In Fig. 4 a-c, the comparisons between the performance of the HOA and GA convergence of the three studied systems are shown. The general remark for the simulations of the whole systems is that the fitness function converged fast and smoothly in the case of using the new proposed algorithm. For the base OPF case,

TABLE 5. Optimal fitness and population values for the base case OPF for system 3.

Generator power (MW) at bus	HOA	GA	HHO [13]
1	25.9569064448638	46.64348288	6.14
4	0	32.60295454	0.02
6	2.79295179374116	38.08212633	9.47
8	0	26.19771312	29.64
10	401.153508538168	272.3710272	418.52
12	86.4024929847601	73.22827184	81.38
15	23.7553765283501	38.00522085	1.53
18	15.5321497214307	34.73950011	41.21
19	22.5286788592375	40.75631948	5.35
24	0	45.96633966	0.89
25	194.038964055319	131.1105628	205.95
26	279.900508903909	217.7297736	286.68
27	15.5852003642891	31.14068180	1.2
31	7.33295615709312	23.00674347	7.28
32	0	50.91634097	13.63
34	7.45998354223770	30.65930124	9.47
36	12.9586665902067	42.57814840	4.02
40	51.9899982657949	36.82208311	13.46
42	45.5877409328148	42.65108000	17.48
46	19.1512252820705	31.82180145	16.89
49	194.368094547667	125.4309740	201.58
54	49.5997668701826	52.65948198	52.46
55	32.5979296835137	41.29486450	12.001
56	33.3989030918837	51.30437655	33.6
59	149.965921221199	111.2667226	155.42
61	148.357681279316	113.5439380	156.8
62	0	50.44757113	1.63E-05
65	352.842910139785	288.9085804	354.2
66	350.053226789271	229.0812981	351.75
69	454.548251958255	314.3999459	458.96
70	0	45.36362440	38.86
72	0	40.87926448	1.61E-05
73	3.9071177433e-11	42.24423377	4.62
74	16.1400267200474	55.42070675	9.96
76	19.1941898860551	40.80981321	5.31
77	0	43.01983463	39.73
80	432.577039496406	276.9136770	373.61
85	0	39.54586246	6.01E-06
87	3.62153149115355	13.28940124	3.54
89	495.596247101245	328.0306755	506.89
90	0	41.98526830	5.70E-07
91	0	48.71205557	4.05
92	3.0472483391e-13	45.01746368	2.11E-05
99	0	45.43678927	29.26
100	231.381382531255	157.5240341	232.49
103	38.3907670990906	35.41607758	37.89
104	8.2367412732e-12	42.73532186	6.49
105	4.37502795687037	38.51249849	2.82
107	29.4981684339238	40.73271291	22.52
110	6.67915923130552	38.59811299	30.76
111	35.0740731619637	44.21429573	31.5
112	40.8927288763138	47.27614646	10.07
113	0	41.84418476	3.75
116	2.7195183515e-12	47.72560846	7.61E-06
Min cost($/hr)	130160.197435109	135957.3447	130599.75

the percentage reductions in the fuel cost of the 30-, 57-, 118-bus systems obtained due to the employment of the HOA by solving the OPF are 0.8%, 0.04%, and 4.26 %, respectively. It is observed that the HOA performs better when the system becomes larger.

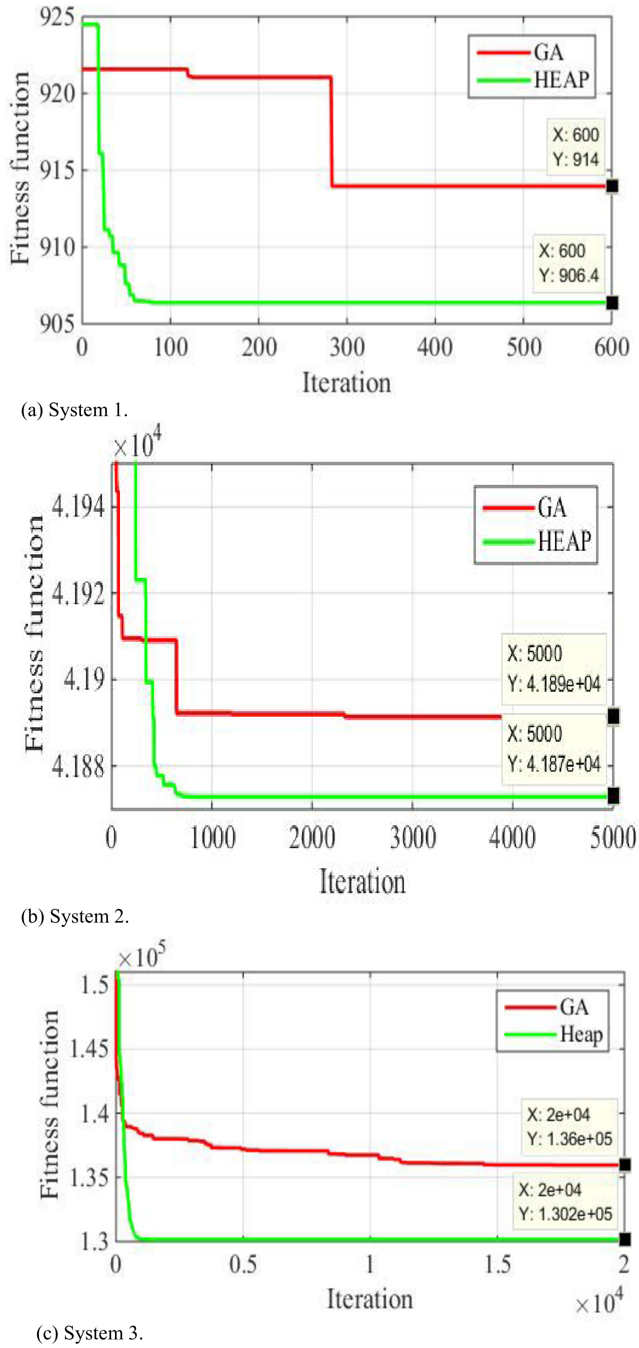

FIGURE 4. Convergence of the objective function for: (a) System 1, (b) System 2, (c) System 3.

TABLE 6. Optimal locations for PV and wind energy sources.

Test system	30-bus	57-bus	118-bus
Optimal PV location	4	47	114
Optimal wind farm location	21	48	15

B. OPTIMAL ALLOCATION OF PV PANEL AND WIND FARM

The second stage of this research is to find an optimal bus at which a PV panel can be placed and the same for a

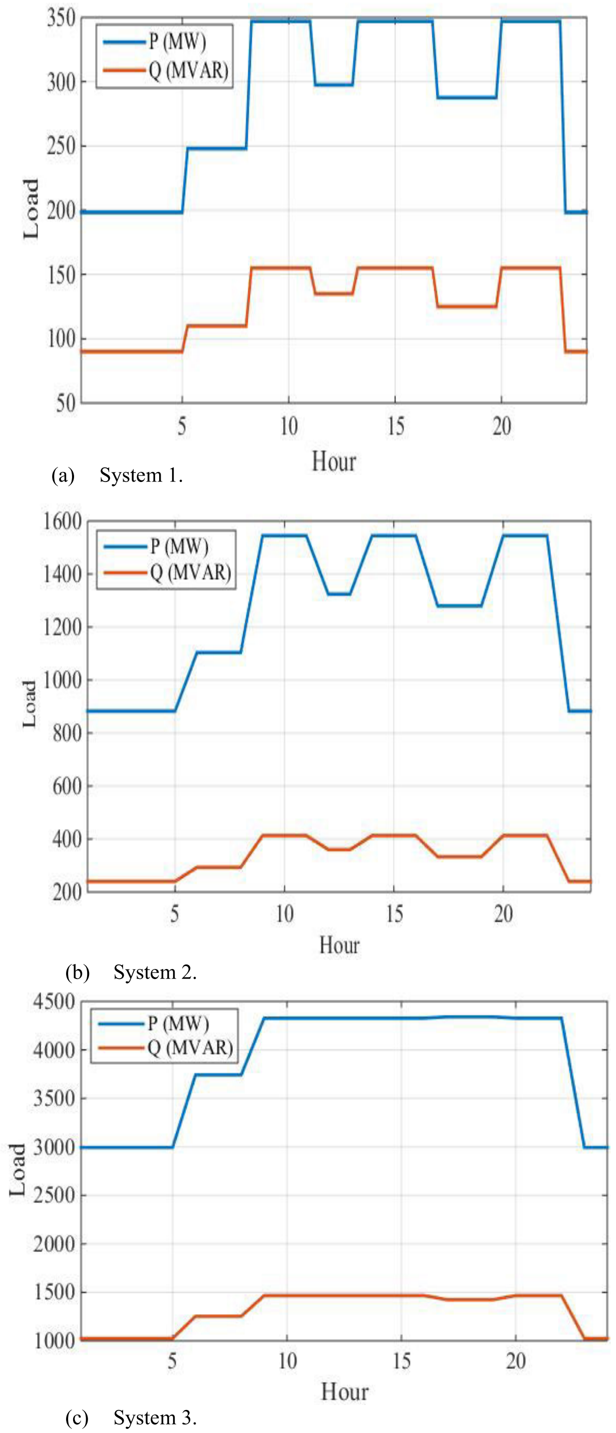

FIGURE 5. Load Curves of the IEEE test systems, (a) System 1, (b) System 2, (c) System 3.

wind turbine. The optimal bus is the bus that corresponds to a minimum fuel cost when performing the OPF problem considering insertion of the PV panels at the whole buses one at a time. This is studied for the three aforementioned IEEE bus test systems, 30-bus, 57-bus, and 118-bus systems. The SFO algorithm is employed for this task in case of the IEEE 30-bus system. Meanwhile, the HHO algorithm is the one which is employed for this task in case of the IEEE 57-bus system and the 118-bus system. The optimal bus for a PV panel only is targeted first. Then, the optimal bus for a wind farm only is targeted. Table 6 presents the results of the simulations of this stage, which is the optimal locations for the PV panel and the wind farm in the case of each test system. These locations are used in the OPF with renewable energy sources (RES) and variable loading conditions which is the next stage of the research and they are presented in detail in the following section. The PV and wind energy sources are considered stepped negative loads and the uncertainty is neglected in this study for simplicity [33]–[36].

TABLE 7. Scenarios of OPF.

Scenario No.	Test system	PV panel at bus	Wind farm at bus
1	30-bus system	-	-
	57-bus system	-	-
	118-bus system	-	-
2	30-bus system	4	-
	57-bus system	47	-
	118-bus system	114	-
3	30-bus system	-	21
	57-bus system	-	48
	118-bus system	-	15
4	30-bus system	4	21
	57-bus system	47	48
	118-bus system	114	15

TABLE 8. Simulation time taken by the HOA in the four studied scenarios.

Test System	Scenario	Simulation time (s)	
		HOA	GA
IEEE 30-bus	None	2723.75	1656.4
	PV	2167.03	2209.975
	Wind	1162.48	1518.71
	Hybrid	1817.68	2232.21
IEEE 57-bus	None	2028.19	2958.869
	PV	1446.36	2319.9102
	Wind	1800.79	2605.3106
	Hybrid	2304.13	2578.7148
IEEE 118-bus	None	1840.2	2506.93035
	PV	3205.57	4666.767
	Wind	6862.8	4697.514
	Hybrid	3921.12	4739.019

TABLE 9. Reactive power of the generators:30-bus system.

Generator Number	Generator at bus	Generator reactive power
1	1	-15.75247491
2	2	51.94564166
3	5	27.92964763
4	8	26.85483047
5	11	15.37332392
6	13	8.594153394

TABLE 10. Reactive power of the generators:57-bus system.

Generator Number	Generator at bus	Generator reactive power
1	1	190.271881
2	2	-28.70704164
3	3	-6.198962902
4	6	-21.68044383
5	8	61.03808859
6	9	-19.26355139
7	12	108.1101916

C. OPF WITH RES PENETRATION AND VARIABLE LOADING CONDITIONS

In the final stage of the study, the OPF single objective optimization problem is targeted with various scenarios and loading conditions. These scenarios represent the integration of the PV panel only, the wind farm only, both PV panel and the wind farm with the systems under study. The loading conditions are not constant over the day, but they change their values hourly. All scenarios and loading variation are tested for the three systems, 30-bus, 57-bus, and 118-bus systems. The order of performing the OPF scenarios is as follows: (1) The OPF is performed firstly without insertion of PV panels or wind farms, only the load is changing hourly. (2) The OPF is performed with only PV panel is added to the previously determined optimal bus for the whole test systems. (3) The OPF is performed with only wind farm is added to the previously selected optimal bus for each test system. (4) The last scenario is to perform the OPF with including PV panel and wind farm in addition to the hourly changing loads for the three test systems. The summary of these scenarios is presented in Table 7. The comparisons for all scenarios are presented between the newly proposed HOA and the well-established GA. The load curves of the systems under study are shown in Fig. 5 a-c.

In scenario 1, The results obtained by the newly developed HOA and GA are close together in the 30-bus system, but the HOA obtained better results in the 57-bus and the 118-bus systems, especially during the hours of high loading condition. The HOA results present a percentage reduction of 1.018% compared with the GA results when testing the 30-bus system. The percentages of reduction are about 0.7% and 9% of the 57- bus and 118- bus systems, respectively. The hourly comparisons between the HOA and GA in the fuel cost of the three test systems are shown in Fig. 6 a-c.

In scenario 2, the PV panel is added to bus 4 in the 30-bus system, while it is added to bus 47 in the 57-bus system, and it is added to bus 114 in the 118-bus system. The HOA resulted in a percentage reduction of 1.015% compared with the GA results when testing the 30-bus system. The percentages of reduction are about 3.3% and 6.2% of the 57- bus and 118- bus systems, respectively. The hourly comparisons between the HOA and GA of the fuel cost of the three test systems are shown in Fig. 7 a-c.

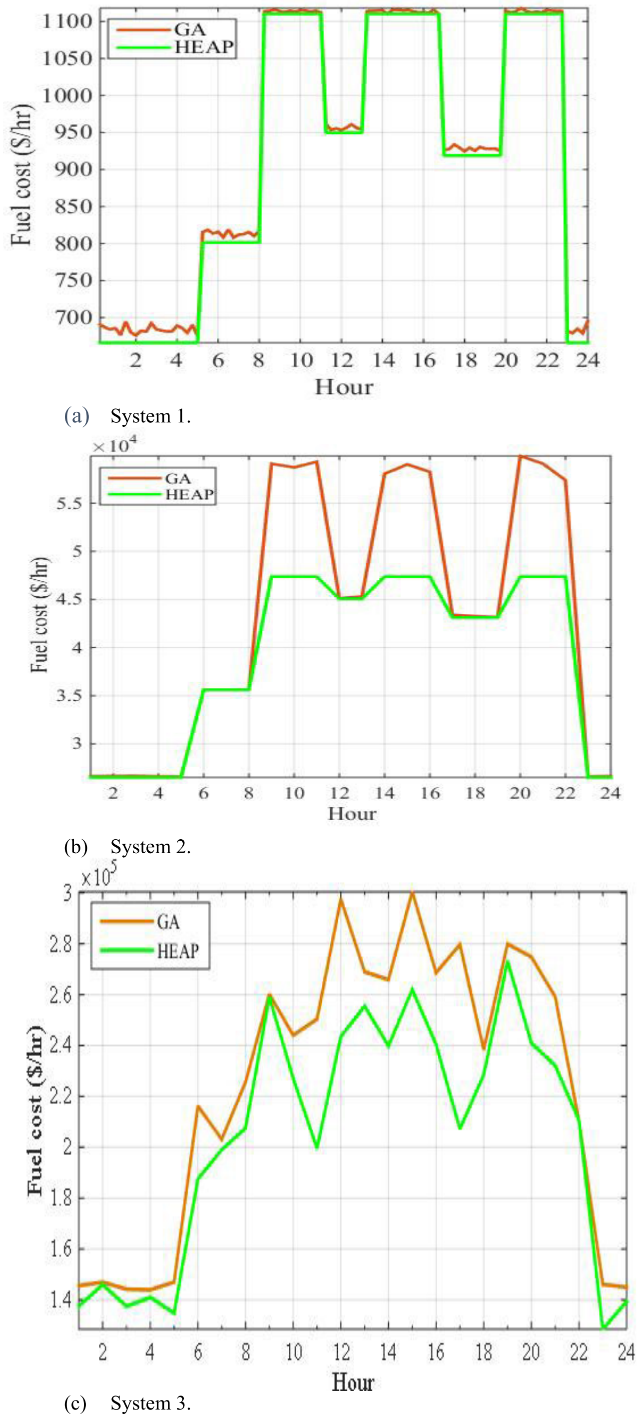

FIGURE 6. Scenario 1 results for (a) System 1, (b) System 2, (c) System 3.

In scenario 3, the wind farm is added to bus 21 in the 30-bus system, while it is added to bus 48 in the 57-bus system, and it is added to bus 15 in the 118-bus system. The HOA resulted in a percentage reduction of 1.33% compared with the GA results when testing the 30-bus system. The percentages of

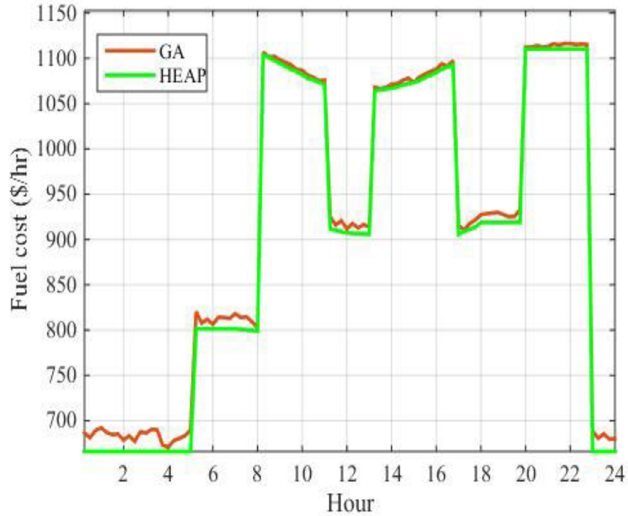

(a) System 1.

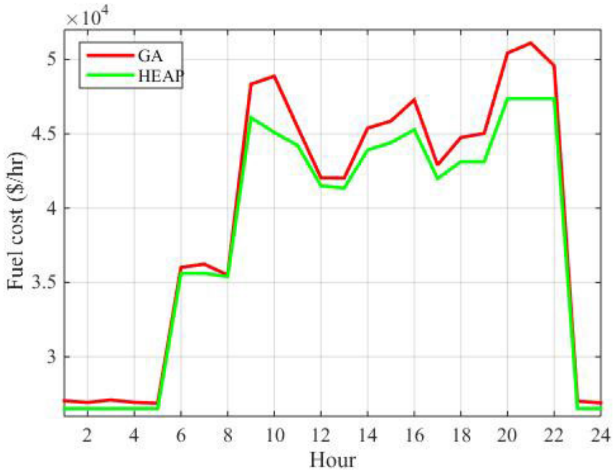

(b) System 2.

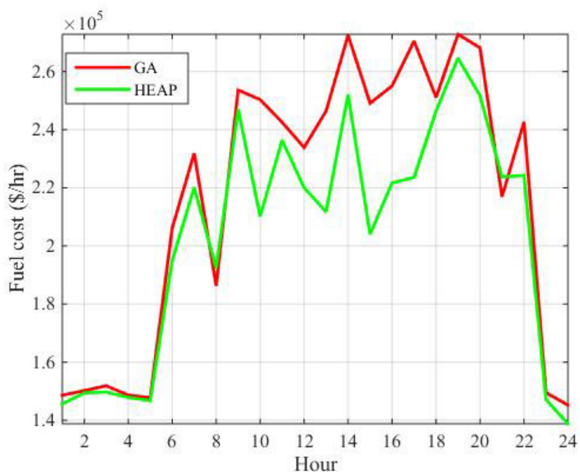

(c) System 3.

FIGURE 7. Scenario 2 results for, (a) System 1, (b) System 2, (c) System 3.

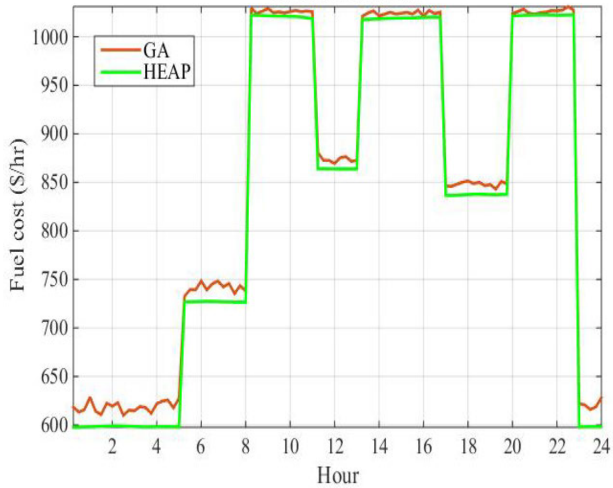

(a) System 1.

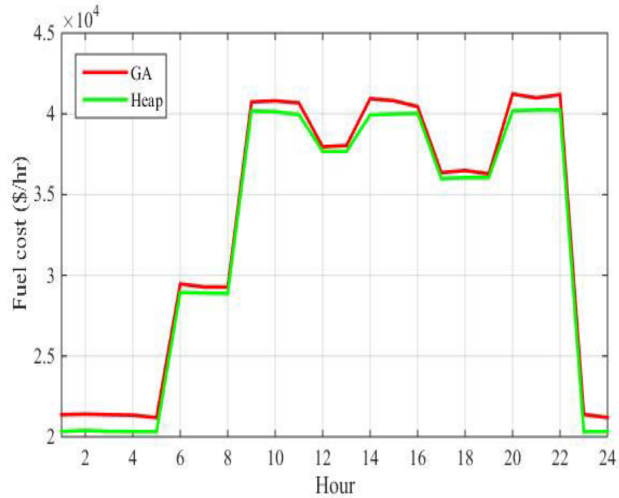

(b) System 2.

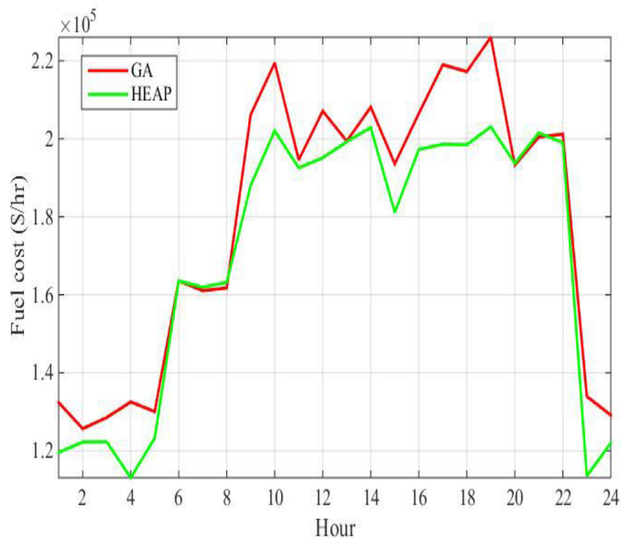

(c) System 3.

FIGURE 8. Scenario 3 results for, (a) System 1, (b) System 2, (c) System 3.

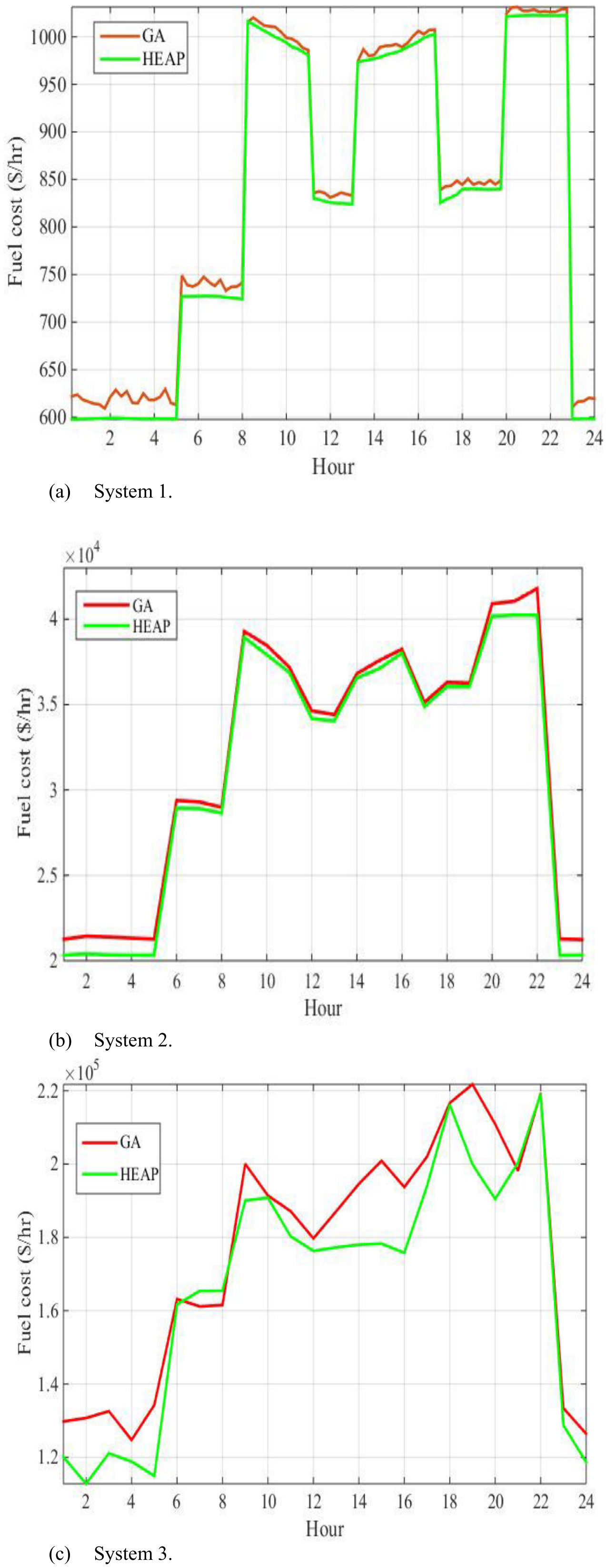

FIGURE 9. Scenario 4 results for, (a) System 1, (b) System 2, (c) System 3.

TABLE 11. Reactive power of the generators:118-bus system.

Generator Number	Generator at bus	Generator reactive power
1	1	-11.2476704
2	4	-12.45792307
3	6	15.28730561
4	8	39.85669482
5	10	-59.23663371
6	12	90.2374437
7	15	-1.672212604
8	18	23.27792099
9	19	-21.24316881
10	24	-14.92947761
11	25	49.31223299
12	26	4.057031498
13	27	-2.637959913
14	31	32.34997513
15	32	-18.48815206
16	34	-23.82700753
17	36	3.757068701
18	40	8.7382155
19	42	21.62167896
20	46	-7.224990196
21	49	97.68177363
22	54	2.107681508
23	55	-4.948186924
24	56	-15.27853212
25	59	77.78394618
26	61	-40.67549821
27	62	0.994742494
28	65	68.1430576
29	66	3.577486473
30	69	-78.25962196
31	70	5.983671988
32	72	-11.1768749
33	73	9.599729279
34	74	-11.96799702
35	76	-2.282364886
36	77	7.695871815
37	80	107.1652732
38	85	-6.970082711
39	87	11.09654834
40	89	5.172437875
41	90	58.74559434

TABLE 11. ***(Continued.)*** **Reactive power of the generators:118-bus system.**

42	91	-12.87985349
43	92	-24.65757799
44	99	-17.53594418
45	100	90.92458963
46	103	67.14758811
47	104	0.603183536
48	105	-21.68808174
49	107	-3.574086159
50	110	-1.510603936
51	111	-1.602239182
52	112	23.91705664
53	113	5.866585957
54	116	53.43720708

reduction are 2.13% and 4.8% of the 57- bus and 118- bus systems, respectively. The hourly comparisons between the HOA and GA of the fuel cost of the three test systems are shown in Fig. 8 a-c.

In scenario 4, PV panel is added to bus 4 and the wind farm is added to bus 21 in the 30-bus system, while they are added to buses 47 and 48 respectively in the 57-bus system, and they are added to buses 114, and 15 respectively in the 118-bus system. The HOA resulted in a percentage reduction of 1.36% compared with GA when testing the 30-bus system. The percentages of reduction are 1.94% and 4.85% of the 57- bus and 118- bus systems, respectively. The hourly comparisons between the HOA and GA of the fuel cost of the three test systems are shown in Fig. 9 a-c. The simulation times taken by the proposed HOA and the GA algorithms for the studied scenarios are summarized in Table 8.

From the results, it can be observed that using the proposed algorithm led to improvement in results of the objective function in the base case of the OPF problem by (0.84 – 1.227) % for the first test system, (0.00038 – 0.93) % for the second test system, (0.33 – 4.45) % for the third test system. On the other hand, when comparing the simulation time, it can be seen that the HOA is the fastest in the third test system, but it came second in speed after the PSO in the first and second test systems.

For further considerations and future works, energy storage is now included in Active Network Management schemes. Dynamic optimal power flow is an extension of OPF to cover multiple time periods [37]. Moreover, demand response (DR) represents an important part of the electrical power network operation. Also, Smart grids will increase the utilization of DR [37]. DR is also implemented for planning decisions [39]. On the other hand, In [40], planning for optimal allocation

TABLE 12. **Transmission Line apparent power:30-bus system.**

Transmission Line Number	From bus	To bus	Apparent Power
1	1	2	155.4198749
2	1	3	73.57224631
3	2	4	34.07814149
4	3	4	68.85524635
5	2	5	67.34270628
6	2	6	47.53216733
7	4	6	60.4182131
8	5	7	16.63567629
9	6	7	35.55840523
10	6	8	20.64984534
11	6	9	21.59323169
12	6	10	13.21721146
13	9	11	18.33954984
14	9	10	30.20966238
15	4	12	36.84249125
16	12	13	14.76006343
17	12	14	8.401172873
18	12	15	19.91648543
19	12	16	8.546427953
20	14	15	1.882263273
21	16	17	4.566905777
22	15	18	6.570520155
23	18	19	3.193977124
24	19	20	7.004546139
25	10	20	9.437584732
26	10	17	6.634091765
27	10	21	18.82773198
28	10	22	8.990034159
29	21	22	2.225750053
30	15	23	6.349604968
31	22	24	6.759873069
32	23	24	2.70993001
33	24	25	1.600921465
34	25	26	4.261951421
35	25	27	3.775790927
36	28	27	17.77549593
37	27	29	6.410727057
38	27	30	7.284049848
39	29	30	3.752880066
40	8	28	2.638686901
41	6	28	16.60363158

TABLE 13. Transmission Line apparent power:57-bus system.

TABLE 13. *(Continued.)* Transmission Line apparent power:57-bus system.

Transmission Line Number	From bus	To bus	Apparent Power
1	1	2	136.8739806
2	2	3	45.00941586
3	3	4	16.48842256
4	4	5	14.71053677
5	4	6	24.92938294
6	6	7	14.11724613
7	6	8	42.08345953
8	8	9	185.0274771
9	9	10	38.82630026
10	9	11	45.89516423
11	9	12	27.67684097
12	9	13	35.60560815
13	13	14	22.73172213
14	13	15	15.44930954
15	1	15	72.3662944
16	1	16	34.92059111
17	1	17	49.45379966
18	3	15	52.93824921
19	4	18	14.23545414
20	4	18	17.9930532
21	5	6	25.35035905
22	7	8	82.5351172
23	10	12	23.52929624
24	11	13	24.55762068
25	12	13	63.40922753
26	12	16	9.977977937
27	12	17	7.786766182
28	14	15	41.44628518
29	18	19	4.964963418
30	19	20	1.483295923
31	21	20	1.038667679
32	21	22	1.039899265
33	22	23	7.802792852
34	23	24	5.562666445
35	24	25	7.504483663
36	24	25	7.211625764
37	24	26	16.51189922
38	26	27	16.92148904
39	27	28	26.6312403
40	28	29	31.78793109
41	7	29	67.37797222
42	25	30	9.19061985
43	30	31	4.98037579
44	31	32	1.680551292
45	32	33	4.258851593
46	34	32	8.014024285
47	34	35	8.014024287
48	35	36	14.71042321
49	36	37	19.17491121
50	37	38	24.02685148
51	37	39	4.391465499
52	36	40	4.9478077
53	22	38	8.730539415
54	11	41	10.64039751
55	41	42	10.39361214
56	41	43	13.19630125
57	38	44	15.30274417
58	15	45	27.77256046
59	14	46	52.30278549
60	46	47	51.35826105
61	47	48	19.64699809
62	48	49	6.783134971
63	49	50	8.460242599
64	50	51	16.95763841
65	10	51	35.94795015
66	13	49	47.62053925
67	29	52	18.00521162
68	52	53	12.43156727
69	53	54	8.992942564
70	54	55	13.73053989
71	11	43	15.49958321
72	44	45	27.73201239
73	40	56	4.933592651
74	56	41	6.671829826
75	56	42	3.008889965
76	39	57	4.382736333
77	57	56	3.781536498
78	38	49	11.85791416
79	38	48	26.20104069
80	9	55	21.57017417

TABLE 14. Transmission Line apparent power:118-bus system.

Transmission Line Number	From bus	To bus	Apparent Power
1	1	2	16.19516513
2	1	3	30.9526128
3	4	5	99.71527581
4	3	5	58.73353321
5	5	6	79.64963738
6	6	7	29.70911681
7	8	9	407.5454515
8	8	5	323.9646851
9	9	10	405.5035341
10	4	11	56.95215386
11	5	11	69.09270228
12	11	12	38.76901495
13	2	12	32.8936251
14	3	12	14.82682976
15	7	12	11.62982977
16	11	13	33.85633403
17	12	14	15.54407039
18	13	15	4.294273769
19	14	15	8.968240002
20	12	16	9.943628483
21	15	17	87.22825731
22	16	17	17.59960224
23	17	18	65.6883144
24	18	19	23.21768165
25	19	20	4.860452415
26	15	19	19.1683577
27	20	21	19.86884336
28	21	22	34.05890119
29	22	23	45.29636129
30	23	24	25.16990732
31	23	25	160.5869773
32	26	25	91.56689601
33	25	27	130.5033238
34	27	28	31.16349022
35	28	29	15.25529098
36	30	17	219.5263666
37	8	30	96.72403964
38	26	30	192.7490226
39	17	31	24.23857992
40	29	31	12.9805369
41	23	32	79.89905652

TABLE 14. *(Continued.)* Transmission Line apparent power:118-bus system.

42	31	32	28.36791103
43	27	32	14.17317015
44	15	33	8.286524196
45	19	34	10.99537127
46	35	36	7.0228185
47	35	37	32.18743513
48	33	37	19.09545575
49	34	36	23.51082283
50	34	37	98.69644236
51	38	37	219.5282678
52	37	39	31.87189678
53	37	40	21.17277954
54	30	38	78.18586291
55	39	40	3.292341796
56	40	41	18.29234579
57	40	42	11.61224054
58	41	42	20.68399591
59	43	44	9.497327173
60	34	43	9.838973342
61	44	45	25.38097392
62	45	46	32.20846224
63	46	47	26.77766433
64	46	48	15.65541504
65	47	49	19.38179739
66	42	49	40.3626348
67	42	49	40.3626348
68	45	49	47.71072872
69	48	49	35.04195061
70	49	50	49.74450281
71	49	51	63.22495858
72	51	52	27.44528481
73	52	53	10.36197008
74	53	54	15.45672977
75	49	54	35.34191782
76	49	54	34.5760721
77	54	55	4.838700613
78	54	56	10.02162102
79	55	56	12.72330148
80	56	57	20.75981396
81	50	57	32.02095049
82	56	58	6.11921398
83	51	58	15.3456945

TABLE 14. *(Continued.)* **Transmission Line apparent power:118-bus system.**

84	54	59	22.46482219
85	56	59	19.98181451
86	56	59	20.81642898
87	55	59	24.64075774
88	59	60	35.90069486
89	59	61	44.27649726
90	60	61	106.3963528
91	60	62	10.89257588
92	61	62	29.66461859
93	63	59	145.5973309
94	63	64	145.5973309
95	64	61	32.35796689
96	38	65	143.1893783
97	64	65	171.0836627
98	49	66	107.7154963
99	49	66	107.7154963
100	62	66	39.96683491
101	62	67	27.34230267
102	65	66	72.72651769
103	66	67	55.35263873
104	65	68	84.223847
105	47	69	44.90126243
106	49	69	35.81942779
107	68	69	154.5347783
108	69	70	96.91060198
109	24	70	6.862003298
110	70	71	15.06433404
111	24	72	9.98176792
112	71	72	6.455944587
113	71	73	12.26236949
114	70	74	21.37283895
115	70	75	12.31804669
116	69	75	102.6648758
117	74	75	39.67034609
118	76	77	54.11258118
119	69	77	73.77393977
120	75	77	27.20252526
121	77	78	49.86221263
122	78	79	29.05365312
123	77	80	98.17912994
124	77	80	46.19152188
125	79	80	69.07846856

TABLE 14. *(Continued.)* **Transmission Line apparent power:118-bus system.**

126	68	81	73.82285985
127	81	80	73.82285985
128	77	82	25.07300464
129	82	83	25.90721486
130	83	84	17.9936233
131	83	85	27.9360333
132	84	85	25.50348036
133	85	86	19.05640115
134	86	87	15.58164616
135	85	88	36.74445663
136	85	89	57.51638769
137	88	89	85.89202821
138	89	90	55.06868803
139	89	90	104.6037201
140	90	91	12.02313656
141	89	92	146.953018
142	89	92	46.51037632
143	91	92	18.12280678
144	92	93	37.466052
145	92	94	33.10581586
146	93	94	27.93946937
147	94	95	37.6627461
148	80	96	34.44477696
149	82	96	16.14900588
150	94	96	16.74222185
151	80	97	42.04694302
152	80	98	30.55792801
153	80	99	23.26507845
154	92	100	19.18570511
155	94	100	47.16937746
156	95	96	21.1318425
157	96	97	25.84866162
158	98	100	9.020038799
159	99	100	23.13008622
160	100	101	20.7888911
161	92	102	27.18203091
162	101	102	22.87368762
163	100	103	73.24426545
164	100	104	40.3791519
165	103	104	31.24425523
166	103	105	35.7526262
167	100	106	43.00467444

TABLE 14. *(Continued.)* **Transmission Line apparent power:118-bus system.**

168	104	105	26.60872171
169	105	106	11.7954862
170	105	107	13.07257313
171	105	108	7.755638906
172	106	107	9.822268319
173	108	109	5.841663009
174	103	110	32.7538144
175	109	110	7.871511259
176	110	111	35.1106505
177	110	112	31.77330784
178	17	113	9.817448254
179	32	113	16.16327704
180	32	114	9.267364369
181	27	115	22.29989701
182	114	115	0.89797348
183	68	116	196.4423459
184	12	117	21.54065923
185	75	118	44.80351045
186	76	118	11.72591879

TABLE 15. **Generator capacity limits of 30-bus system.**

Gen. No.	Gen. at bus	P_{max} (MW)
1	1	400
2	2	80
3	5	50
4	8	35
5	11	30
6	13	40

TABLE 16. **Generator capacity limits of 57-bus system.**

Gen. No.	Gen. at bus	P_{max} (MW)
1	1	576
2	2	100
3	3	140
4	6	100
5	8	550
6	9	100
7	12	410

TABLE 17. **Generator capacity limits of 118-bus system.**

Gen. No.	Gen. at bus	P_{max} (MW)
1	1	100
2	4	100
3	6	100
4	8	100
5	10	550
6	12	185
7	15	100
8	18	100
9	19	100
10	24	100
11	25	320
12	26	414
13	27	100
14	31	107
15	32	100
16	34	100
17	36	100
18	40	100
19	42	100
20	46	119
21	49	304
22	54	148
23	55	100
24	56	100
25	59	255
26	61	260
27	62	100
28	65	491
29	66	492
30	69	805
31	70	100
32	72	100
33	73	100
34	74	100
35	76	100
36	77	100
37	80	577
38	85	100
39	87	104
40	89	707
41	90	100

TABLE 17. ***(Continued.)*** **Generator capacity limits of 118-bus system.**

42	91	100
43	92	100
44	99	100
45	100	352
46	103	140
47	104	100
48	105	100
49	107	100
50	110	100
51	111	136
52	112	100
53	113	100
54	116	100

of parking lot-based charging infrastructures to facilitate the efficient integration of plug-in electric vehicles is presented.

V. CONCLUSION

This article has proposed an application of the newly developed HOA in solving one of the most vital problems in the field of electric power systems, the OPF problem. The simulation is performed on the standard test systems, the IEEE 30-bus, 57-bus, and 118-bus systems. In the second part of the research, The SFO and HHO algorithms are employed to select optimal buses for inserting PV panel and wind farm into the systems under study. As a final stage, the proposed HOA is used to solve the OPF problem considering different scenarios of renewable power sources integration with the power systems and varying load conditions in the three systems. The simulation results have confirmed the validity, and robustness of the newly developed HOA method compared with the results obtained by GA. The HOA method has extensively shown a higher speed and smoother convergence of the fitness function besides its simplicity in computations and implementation. The application of the HOA has resulted in a 4% reduction in fuel cost for the base case OPF. Meanwhile, in the different scenarios, the HOA has demonstrated a percentage reduction in the daily costs by (0.7-9%) compared with that achieved by the GA results. So, it is recommended to consider using the HOA method in further applications in the field of power system simulations such as smart grids in the future works.

REFERENCES

[1] Q. Hou, E. Du, N. Zhang, and C. Kang, "Impact of high renewable penetration on the power system operation mode: A data-driven approach," *IEEE Trans. Power Syst.*, vol. 35, no. 1, pp. 731–741, Jan. 2020, doi: 10.1109/TPWRS.2019.2929276.

[2] A. A. Nazari, R. Keypour, M. H. Beiranvand, and N. Amjady, "A decoupled extended power flow analysis based on Newton-Raphson method for islanded microgrids," *Int. J. Electr. Power Energy Syst.*, vol. 117, May 2020, Art. no. 105705, doi: 10.1016/j.ijepes.2019.105705.

[3] W. Lu, M. Liu, S. Lin, and L. Li, "Fully decentralized optimal power flow of multi-area interconnected power systems based on distributed interior point method," *IEEE Trans. Power Syst.*, vol. 33, no. 1, pp. 901–910, Jan. 2018, doi: 10.1109/TPWRS.2017.2694860.

[4] F. E. Fernandes Junior and G. G. Yen, "Particle swarm optimization of deep neural networks architectures for image classification," *Swarm Evol. Comput.*, vol. 49, pp. 62–74, Sep. 2019, doi: 10.1016/j.swevo.2019.05.010.

[5] M. H. Nadimi-Shahraki, S. Taghian, and S. Mirjalili, "An improved grey wolf optimizer for solving engineering problems," *Expert Syst. Appl.*, vol. 166, Mar. 2021, Art. no. 113917, doi: 10.1016/j.eswa.2020.113917.

[6] M. A. M. Shaheen, H. M. Hasanien, and A. Alkuhayli, "A novel hybrid GWO-PSO optimization technique for optimal reactive power dispatch problem solution," *Ain Shams Eng. J.*, Aug. 2020, doi: 10.1016/j.asej.2020.07.011.

[7] I. Gungor, B. G. Emiroglu, A. C. Cinar, and M. S. Kiran, "Integration search strategies in tree seed algorithm for high dimensional function optimization," *Int. J. Mach. Learn. Cybern.*, vol. 11, no. 2, pp. 249–267, Feb. 2020, doi: 10.1007/s13042-019-00970-1.

[8] S. Gupta and K. Deep, "Improved sine cosine algorithm with crossover scheme for global optimization," *Knowl.-Based Syst.*, vol. 165, pp. 374–406, Feb. 2019, doi: 10.1016/j.knosys.2018.12.008.

[9] M. A. M. Shaheen, H. M. Hasanien, S. F. Mekhamer, and H. E. A. Talaat, "Optimal power flow of power systems including distributed generation units using sunflower optimization algorithm," *IEEE Access*, vol. 7, pp. 109289–109300, 2019, doi: 10.1109/ACCESS.2019.2933489.

[10] G. F. Gomes and F. A. de Almeida, "Tuning Metaheuristic algorithms using mixture design: Application of sunflower optimization for structural damage identification," *Adv. Eng. Softw.*, vol. 149, Nov. 2020, Art. no. 102877, doi: 10.1016/j.advengsoft.2020.102877.

[11] A. A. Z. Diab, H. M. Sultan, T. D. Do, O. M. Kamel, and M. A. Mossa, "Coyote optimization algorithm for parameters estimation of various models of solar cells and PV modules," *IEEE Access*, vol. 8, pp. 111102–111140, 2020, doi: 10.1109/ACCESS.2020.3000770.

[12] H. Chen, S. Jiao, M. Wang, A. A. Heidari, and X. Zhao, "Parameters identification of photovoltaic cells and modules using diversification-enriched harris hawks optimization with chaotic drifts," *J. Cleaner Prod.*, vol. 244, Jan. 2020, Art. no. 118778, doi: 10.1016/j.jclepro.2019.118778.

[13] M. A. M. Shaheen, H. M. Hasanien, S. F. Mekhamer, and H. E. A. Talaat, "Optimal power flow of power networks with penetration of renewable energy sources by harris hawks optimization method," in *Proc. 2nd Int. Conf. Smart Power Internet Energy Syst. (SPIES)*, Sep. 2020, pp. 537–542, doi: 10.1109/SPIES48661.2020.9242932.

[14] A. M. Hussien, S. F. Mekhamer, and H. M. Hasanien, "Cuttlefish optimization algorithm based optimal PI controller for performance enhancement of an autonomous operation of a DG system," in *Proc. 2nd Int. Conf. Smart Power Internet Energy Syst. (SPIES)*, Sep. 2020, pp. 293–298, doi: 10.1109/SPIES48661.2020.9243093.

[15] R. N. Kalaam, S. M. Muyeen, A. Al-Durra, H. M. Hasanien, and K. Al-Wahedi, "Optimisation of controller parameters for grid-tied photovoltaic system at faulty network using artificial neural network-based cuckoo search algorithm," *IET Renew. Power Gener.*, vol. 11, no. 12, pp. 1517–1526, Oct. 2017, doi: 10.1049/iet-rpg.2017.0040.

[16] O. S. Elazab, H. M. Hasanien, M. A. Elgendy, and A. M. Abdeen, "Parameters estimation of single-and multiple-diode photovoltaic model using whale optimisation algorithm," *IET Renew. Power Gener.*, vol. 12, no. 15, pp. 1755–1761, Nov. 2018, doi: 10.1049/iet-rpg.2018.5317.

[17] H. M. Hasanien, "Gravitational search algorithm-based optimal control of archimedes wave swing-based wave energy conversion system supplying a DC microgrid under uncertain dynamics," *IET Renew. Power Gener.*, vol. 11, no. 6, pp. 763–770, May 2017, doi: 10.1049/iet-rpg.2016.0677.

[18] M. A. M. Shaheen, D. Yousri, A. Fathy, H. M. Hasanien, A. Alkuhayli, and S. M. Muyeen, "A novel application of improved marine predators algorithm and particle swarm optimization for solving the ORPD problem," *Energies*, vol. 13, no. 21, p. 5679, Oct. 2020, doi: 10.3390/en13215679.

[19] H. M. Hasanien and A. A. El-Fergany, "Salp swarm algorithm-based optimal load frequency control of hybrid renewable power systems with communication delay and excitation cross-coupling effect," *Electr. Power Syst. Res.*, vol. 176, Nov. 2019, Art. no. 105938, doi: 10.1016/j.epsr.2019.105938.

[20] L. Abualigah, M. Shehab, M. Alshinwan, and H. Alabool, "Salp swarm algorithm: A comprehensive survey," *Neural Comput. Appl.*, vol. 15, pp. 1–21, Nov. 2019, doi: 10.1007/s00521-019-04629-4.

[21] A. A. El-Fergany and H. M. Hasanien, "Salp swarm optimizer to solve optimal power flow comprising voltage stability analysis," *Neural Comput. Appl.*, vol. 32, no. 9, pp. 5267–5283, May 2020, doi: 10.1007/s00521-019-04029-8.

[22] O. S. Elazab, M. Debouza, H. M. Hasanien, S. M. Muyeen, and A. Al-Durra, "Salp swarm algorithm-based optimal control scheme for LVRT capability improvement of grid-connected photovoltaic power plants: Design and experimental validation," *IET Renew. Power Gener.*, vol. 14, no. 4, pp. 591–599, Mar. 2020, doi: 10.1049/iet-rpg.2019.0726.

[23] A. H. Halim, I. Ismail, and S. Das, "Performance assessment of the metaheuristic optimization algorithms: An exhaustive review," *Artif. Intell. Rev.*, vol. 7, pp. 1–87, Oct. 2020, doi: 10.1007/s10462-020-09906-6.

[24] Q. Askari, M. Saeed, and I. Younas, "Heap-based optimizer inspired by corporate rank hierarchy for global optimization," *Expert Syst. Appl.*, vol. 161, Dec. 2020, Art. no. 113702, doi: 10.1016/j.eswa.2020.113702.

[25] M. Mousa, M. M. Salah, F. Z. Amer, A. Saeed, and R. I. Mubarak, "High efficiency tandem Perovskite/CIGS solar cell," in *Proc. 2nd Int. Conf. Smart Power Internet Energy Syst. (SPIES)*, Sep. 2020, pp. 224–227, doi: 10.1109/SPIES48661.2020.9242927.

[26] M. A. Soliman, H. M. Hasanien, H. Z. Azazi, E. E. El-kholy, and S. A. Mahmoud, "Hybrid ANFIS-GA-based control scheme for performance enhancement of a grid-connected wind generator," *IET Renew. Power Gener.*, vol. 12, no. 7, pp. 832–843, May 2018, doi: 10.1049/iet-rpg.2017.0576.

[27] M. A. Soliman, H. M. Hasanien, S. Alghuwainem, and A. Al-Durra, "Symbiotic organisms search algorithm-based optimal control strategy for efficient operation of variable-speed wind generators," *IET Renew. Power Gener.*, vol. 13, no. 14, pp. 2684–2692, Oct. 2019, doi: 10.1049/iet-rpg.2019.0834.

[28] H. Li, X. Xie, A. McDonald, Z. Chai, T. Yang, Y. Wu, and W. Yang, "Cost and reliability optimization of modular multilevel converter with hybrid submodule for offshore DC wind turbine," *Int. J. Electr. Power Energy Syst.*, vol. 120, Sep. 2020, Art. no. 105994, doi: 10.1016/j.ijepes.2020.105994.

[29] F. Islam, H. Hasanien, A. Al-Durra, and S. M. Muyeen, "A new control strategy for smoothing of wind farm output using short-term ahead wind speed prediction and flywheel energy storage system," in *Proc. Amer. Control Conf. (ACC)*, Jun. 2012, pp. 3026–3031, doi: 10.1109/ACC.2012.6315503.

[30] A. Parida and B. Subudhi, "Modified leaky LMS-based control strategy for reliable operation of single-stage three-phase grid-tied PV system," *IET Renew. Power Gener.*, vol. 14, no. 9, pp. 1453–1462, Jul. 2020, doi: 10.1049/iet-rpg.2019.0776.

[31] G. Wu, C. Zhang, C. Cai, K. Yang, and K. Shi, "Uncertainty prediction on the angle of attack of wind turbine blades based on the field measurements," *Energy*, vol. 200, Jun. 2020, Art. no. 117515, doi: 10.1016/j.energy.2020.117515.

[32] MATPOWER. *The Newton-Raphson Method*. Accessed: Jan. 2020. [Online]. Available: http://www.pserc.cornell.edu/matpower

[33] S. S. Reddy, "Optimal scheduling of thermal-wind-solar power system with storage," *Renew. Energy*, vol. 101, pp. 1357–1368, Feb. 2017.

[34] S. Surender Reddy, P. R. Bijwe, and A. R. Abhyankar, "Optimal posturing in day-ahead market clearing for uncertainties considering anticipated real-time adjustment costs," *IEEE Syst. J.*, vol. 9, no. 1, pp. 177–190, Mar. 2015, doi: 10.1109/JSYST.2013.2265664.

[35] S. S. Reddy, V. Sandeep, and C. M. Jung, "Review of stochastic optimization methods for smart grid," *Frontiers Energy*, vol. 11, no. 2, pp. 197–209, 2017.

[36] S. S. Reddy, D. of Railroad, and R. o. K. Electrical EngineeringWoosong UniversityDaejeon-300718, "Optimization of renewable energy resources in hybrid energy systems," *J. Green Eng.*, vol. 7, no. 1, pp. 43–60, 2017, doi: 10.13052/jge1904-4720.7123.

[37] S. Gill, I. Kockar, and G. W. Ault, "Dynamic optimal power flow for active distribution networks," *IEEE Trans. Power Syst.*, vol. 29, no. 1, pp. 121–131, Jan. 2014, doi: 10.1109/TPWRS.2013.2279263.

[38] J. Medina, N. Muller, and I. Roytelman, "Demand response and distribution grid operations: Opportunities and challenges," *IEEE Trans. Smart Grid*, vol. 1, no. 2, pp. 193–198, Sep. 2010, doi: 10.1109/TSG.2010.2050156.

[39] B. Zeng, J. Feng, N. Liu, and Y. Liu, "Co-optimized parking lot placement and incentive design for promoting PEV integration considering decision-dependent uncertainties," *IEEE Trans. Ind. Informat.*, vol. 17, no. 3, pp. 1863–1872, Mar. 2021, doi: 10.1109/TII.2020.2993815.

[40] B. Zeng, Y. Liu, F. Xu, Y. Liu, X. Sun, and X. Ye, "Optimal demand response resource exploitation for efficient accommodation of renewable energy sources in multi-energy systems considering correlated uncertainties," *J. Cleaner Prod.*, vol. 288, Mar. 2021, Art. no. 125666, doi: 10.1016/j.jclepro.2020.125666.

MOHAMED A. M. SHAHEEN received the B.Sc. and M.Sc. degrees in electrical engineering from Ain Shams University, Faculty of Engineering, Cairo, Egypt, in 2016 and 2020, respectively, where he is currently pursuing the Ph.D. degree. He is currently an Assistant Lecturer with the Future University in Egypt, Faculty of Engineering. His research interests include power systems operation, energy storage systems, and renewable energy systems.

HANY M. HASANIEN (Senior Member, IEEE) received the B.Sc., M.Sc., and Ph.D. degrees in electrical engineering from Ain Shams University, Faculty of Engineering, Cairo, Egypt, in 1999, 2004, and 2007, respectively. From 2008 to 2011, he was a Joint Researcher with the Kitami Institute of Technology, Kitami, Japan. From 2012 to 2015, he was an Associate Professor with the College of Engineering, King Saud University, Riyadh, Saudi Arabia. He is currently a Professor with the Electrical Power and Machines Department, Faculty of Engineering, Ain Shams University. He has authored, coauthored, and edited three books in the field of electric machines and renewable energy. He has published more than 150 papers in international journals and conferences. His biography has been included in *Marquis Who's Who in the world* for its 28 edition, 2011. His research interests include modern control techniques, power systems dynamics and control, energy storage systems, renewable energy systems, and smart grid. He is an Editorial Board Member of *Electric Power Components and Systems Journal*. He is the Subject Editor of the *IET Renewable Power Generation*, *Ain Shams Engineering Journal*, and *Electronics MDPI*. He was awarded the Encouraging Egypt Award for Engineering Sciences in 2012. He was awarded the Institutions Egypt Award for Invention and Innovation of Renewable Energy Systems Development in 2014. He was awarded the Superiority Egypt Award for Engineering Sciences in 2019. He is currently the IEEE PES Egypt Chapter Chair.

AHMED AL-DURRA (Senior Member, IEEE) received the Ph.D. degree in ECE from Ohio State University in 2010. He is currently a Professor with the EECS Department, Khalifa University, UAE. His research interests are applications of control and estimation theory on power systems stability, micro and smart grids, renewable energy systems and integration, and process control. He has one US patent, one edited book, 12 book chapters, and over 210 scientific articles in top-tier journals and refereed international conference proceedings. He has supervised/co-supervised over 25 Ph.D./master's students. He is leading the Energy Systems Control & Optimization Lab under the Advanced Power & Energy Center, an Editor for the IEEE Transactions on Sustainable Energy and IEEE Power Engineering Letters, and an Associate Editor for the IEEE Transactions on Industry Applications, *IET Renewable Power Generation*, and *Frontiers in Energy Research*.